Advanced Energy Conversion Materials
http://ojs.wiserpub.com/index.php/AECM/

UNIVERSAL WISER PUBLISHER

Research Article

Hydrogen Evolution Activity of Platinum Nanoparticles Decorated on Silver Nanowire Networks and Graphite Electrodes

Martina Schwager*, Felix Deuringer, Michael Moser, Johannes Ostermair, Jenni Richter

Department of Applied Sciences and Mechatronics, Munich University of Applied Sciences, Lothstr. 34, 80335 München, Germany
E-mail: martina.schwager@hm.edu

Received: 1 August 2024; **Revised:** 6 September 2024; **Accepted:** 10 September 2024

Abstract: The catalytic activity of graphite (C) and conductive silver nanowire (AgNW) networks coated on glass and graphite substrates with low platinum content towards hydrogen evolution reaction (HER) is reported. The results exhibit that the chronoamperometric electrodeposition of platinum on AgNW substrates results in the formation of spherically shaped nanoparticle agglomerates aligned on the nanowires. Also, platinum doped graphite electrodes with a rough surface showed an efficient distribution of platinum nanoparticles (PtNPs). Studies of the electrocatalytic HER activity as a function of platinum loading indicate that the optimum loading is in the range of 60 µg/cm^2 and further loading results only in a minor reduction of the overpotential. At low Pt content, a synergistic effect of the AgNW network in terms of enhancement of the HER performance was observed. Tafel analysis showed that in the low overpotential region, the Volmer reaction was the rate determining step for the graphite based electrodes. The graphite substrate in conductive connection with the nanowires was shown to significantly boost the hydrogen formation rate.

***Keywords*:** silver nanowire, platinum nanoparticle, hydrogen evolution reaction, graphite, platinum loading, Tafel analysis, electrocatalytic activity

1. Introduction

In the broad field pertaining to sustainable energy generation, hydrogen has assumed a pivotal role as a chemical energy storage medium, particularly in reference to its application in fuel cells, which enable energy generation whereby only heat and water vapor are produced, reducing the emission of greenhouse gases [1-3]. Besides energy applications, hydrogen is widely used in chemical and petroleum industries [4-6]. Currently, hydrogen production primarily relies on thermochemical processes such as hydrocarbon reforming, pyrolysis, coal gasification, and plasma reforming, all of which depend on fossil fuels and result in significant CO_2 emissions [1]. In contrast, technologies based on renewable sources, like electrochemical water splitting, offer the potential to reduce the carbon footprint associated with hydrogen generation. However, the sustainability of these alternative methods hinges on the cleanliness of the production pathway and crucially, on the efficient utilization of renewable energy to avoid high operational costs [7, 8]. A key challenge in the widespread adoption of hydrogen as an energy carrier lies in its efficient production, where catalysts are of central importance in accelerating the hydrogen evolution reaction [9, 10].

Platinum-based catalysts are known to need only very low overpotentials for HER in acidic solutions [11-13]. Nevertheless, the usage of platinum is associated with high costs, making the production of hydrogen with Pt catalysts

DOI: https://doi.org/10.37256/aecm.5220245423

on a large scale economically unfeasible. It is therefore necessary to reduce the proportion of platinum in catalytic converters without significantly restricting the catalytic effect for HER. It was shown that employing Pt nanoparticles results in a high catalytic HER efficiency even at low loadings [14, 15]. PtNPs exhibit a high specific surface area and their excellent conductivity, as well as hydrogen adsorption and desorption properties, make them particularly suitable for HER [16-19]. The catalytic properties of PtNPs are highly dependent on shape and size as this influences the distribution of different types of catalytically active sites on the NPs [20, 21].

Despite their high HER activity, PtNPs have shown some severe problems. It was observed that, depending on the size of the NPs and the substrate to which they were attached, they tend to agglomerate into larger particles, resulting in a decreased hydrogen formation rate [22, 23]. On certain substrates, even detachment was observed to lower the HER performance [24]. It is therefore an important concern to stabilize nanoparticles on substrates while also maintaining their catalytic effect. To tackle this task novel catalyst materials, including metal oxides like MoO_x/Mo [25] and Pt metal composites, were developed to prevent aggregation and detachment of the nanoparticles [26, 27]. Also, synergistic effects were noticed on composite materials comprising PtNPs, which promoted favorable kinetics of the HER [28-30]. Often carbon based substrates like carbon black [31], graphene [32], carbon nanotubes and nanofibers [33, 34] are used as substrates due to their good stability and conductivity. Additionally, it was shown that structural defects in carbon materials can enhance electrochemical activity due to alteration of the electronic properties at defect sites [35]. The use of nanostructured carbon supports for PtNPs has been the subject of considerable research interest. In addition to their ability to stabilize nanoparticles, these supports have also been shown to provide active sites and exert synergistic effects between the components [36-41].

In the present work, the catalytic activity of platinum nanoparticles immobilized on a rough graphite substrate and deposited on silver nanowires is studied with various platinum loadings. The rough texture of the graphite substrate is anticipated to facilitate extensive dispersion across various morphological sites thereby promoting a uniform distribution of the deposited PtNPs. The diversity of anchoring sites for Pt and AgNWs can enhance catalyst stability by preventing agglomeration of PtNPs and detachment of PtNPs and AgNWs [42].

Silver nanowires, which were applied on glass as well as on graphite substrates, were thermally pretreated to form conductive percolation networks [43]. Scanning electron microscopy (SEM) images were recorded to study the texture of the electrode substrates and in particular the localization and shape of the deposited platinum. By linear sweep voltammetry, the catalytic performance for the HER, which is noticeable in the promotion of a higher hydrogen formation rate with the same applied potential, was studied in 0.5 M H_2SO_4. The electrochemical measurements allow not only the revelation and quantification of the catalytic activity relative to the mass of precious metal used but also the visualization of synergistic effects of the nanostructured substrate in the context of platinum dotation. Kinetic processes and their relationship with electrocatalysis were further investigated using Tafel analysis.

2. Experimental

2.1 *Preparation of platinum decorated AgNW coated electrodes*

AgNW ink purchased from Dycotec (UK) was applied on glass substrates by doctor blade coating and on graphite plates (Phywe, Germany) by dip coating. Average nanowire dimensions are 25 µm in length and 50 nm in diameter. The films were dried under ambient conditions for at least 12 hours to ensure complete evaporation of the solvent. For the production of conductive films, the substrates were in a further step thermally annealed for 45 min at 140 °C. Previous investigations have demonstrated that exposure to temperatures exceeding 300 °C can lead to the disintegration of nanowire morphology [44]. However, given the significantly lower temperature employed in this study for thermal treatment, substantial degradation of the AgNWs is not anticipated.

Platinum decorated electrodes were prepared with graphite and AgNW coated graphite (C/AgNW), as well as AgNW coated glass substrates, using 5 mM H_2PtCl_6 (Merck, Germany) in an acidic solution with 1 M HCl (Merck, Germany). Before the deposition of Pt and AgNW, the graphite substrates were treated in an ultrasonic bath of acetone for 5 minutes. Chronoamperometric electrodeposition was conducted at 0.034 V versus RHE, a potential previously demonstrated to minimize hydrogen evolution on Pt loaded electrodes [45]. This potential was selected to optimize the deposition process, ensuring adequate current flow for the fabrication of even the highest loaded electrodes within a 300

second timeframe.

Considerable silver dissolution was observed upon electroless immersion of the AgNW electrodes in the platinum solution for 2 minutes. This phenomenon can be attributed to the strong oxidizing nature of platinum ions, which induce silver oxidation under open-circuit conditions [46]. To preserve the integrity of the silver nanowires, the electrode potential was applied immediately after immersion. This procedure ensured that platinum reduction occurred via electrochemical means rather than through the oxidation of the silver nanowires, thereby maintaining the nanowire structures intact throughout the deposition process. After deposition, the electrodes were gently rinsed with deionized water and dried under ambient conditions. By varying the deposition time, different Pt loadings were obtained.

2.2 *Electrochemical characterization methods*

All the electrochemical measurements were carried out using a calibrated PalmSens4 (PalmSens, Netherlands) at 25 °C and a three electrode electrochemical system. The counter electrode was an inert graphite plate three times larger than the working electrode to minimize the solution resistance. A calibrated Ag/AgCl electrode in 3 M KCl served as a reference electrode whose potential was periodically verified against a further reference electrode.

Linear sweep voltammetry (LSV) was performed in a 0.5 M H_2SO_4 electrolyte with a scan rate of 50 mV/s in the potential range from 0.1 V to -0.37 V vs. RHE. Prior to recording the polarization curves, typically 10 cyclic voltammograms (CV) were taken (50 mV/s) until a stable current voltage curve was obtained over the potential range with a variation of less than 2%. The polarization curves were calibrated according to RHE using the equation $E_{RHE} = E_{Ag/AgCl} + 0.207\ V + 0.059\ V \cdot pH$. The 0.5 M sulfuric acid had a pH value of 0.46.

In a non-faradaic potential region (0.03-0.43 V vs. RHE) the electrochemical double layer capacitance (C_{dl}) of the graphite substrate was determined with cyclic voltammetry measurements using scan rates from 20 to 200 mV/s.

3. Results and discussion

3.1 *Surface characterization*

The topology of the graphite substrate [42, 47], as well as the shape, size and location of the deposited nanoparticles have a strong impact on the catalytic activity of the HER [48]. In particular, the arrangement of the deposited platinum on the AgNWs, which are coated both on the glass and graphite substrate, is expected to be responsible for possible synergistic silver induced effects [49]. The deposition characteristics of the platinum particles were studied using scanning electron microscopy for the different prepared electrodes.

The mass m_{Pt} of deposited Pt under applying a constant potential (0.034 V vs. RHE) was calculated by the charge Q transferred during the deposition time, which is determined by integrating the current density i and considering the 4 electrons needed for the reduction of Pt^{4+}. With the Faraday constant F and the molar mass M_{Pt} the platinum loading is determined according to Eq. 1

$$m_{Pt} = \frac{Q}{4F} M_{Pt} = \frac{\int idt}{4F} M_{Pt} \tag{1}$$

The metal loadings for the distinct electrode materials, divided by the geometric area that was immersed in the platinum acid solution, are presented in Table 1. Figure 1 depicts SEM images of electrodeposited Pt on various substrates, each with two different view fields.

The AgNWs in the SEM images Figure 1a and b show a statistical non-directional distribution of the nanowires on the surface without preferred orientation. Thermal post-treatment welded the intersections of the wires and a percolation network with direction-independent conductivity was obtained. Along individual silver nanowires, nanoparticles can be clearly recognized. The nanoparticles are not evenly distributed along the length of the wires, but most of them are preferably lined up directly one behind the other.

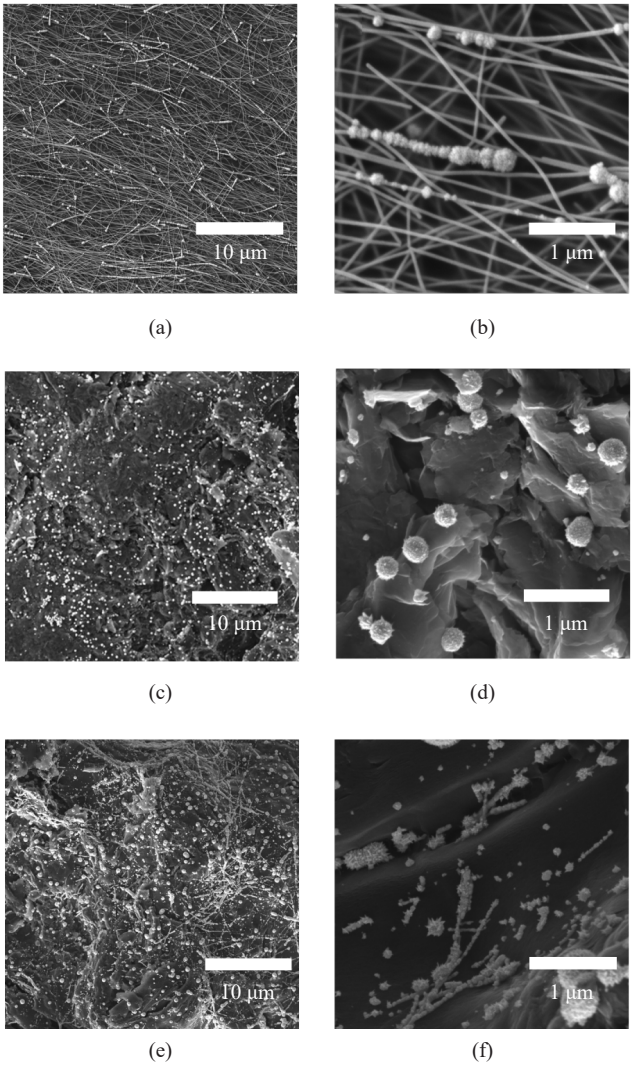

Figure 1. SEM micrographs of electrodeposited Pt nanoparticles: a) Pt on AgNW coated glass substrate (m_{Pt} = 28 µg/cm^2), c) Pt on graphite (m_{Pt} = 47 µg/cm^2), e) Pt on AgNW coated graphite (m_{Pt} = 66 µg/cm^2). b), d) and f) show higher magnifications of a), c) and e) respectively

A significant proportion of nanowires exhibit larger nanoparticles at their termini compared to those along their lengths, with maximum particle dimensions reaching approximately 250 nm. This morphological trend suggests a size-limited growth mechanism, where particle formation is preferentially initiated at wire ends. Detailed analysis of the magnified image (Figure 1b) reveals that the observed structures are agglomerates composed of coalesced particles ranging from approximately 10 to 20 nm in diameter. Such a formation of secondary Pt structures consisting of aggregated particles (30-50 nm) has been observed in the case of electrodeposited Pt on glassy carbon [50]. The more spherical agglomerates are attributed to the low current densities between -0.3 and -1.2 mA/cm^2 that occurred at the applied potential of 0.034 V vs. RHE. Previous studies have indicated that low current densities below -1.5 mA/cm^2 are conducive to the formation of spheres [51, 52].

In Figure 1c the graphite substrate with its coarse surface texture illustrates well distributed nanoparticles preferentially located on top of the surface and less in recesses or pores. The enlarged image (Figure 1d) clearly reveals that these particles are more dendritic shaped which can be attributed to the more negative current density during the deposition (-1.9 mA/cm^2) [52].

Figure 1e shows that the deposition has taken place both on the graphite and on the nanowires. In contrast to the pure silver nanowire network (Figure 1a), the platinum forms almost a complete shell around the nanowire core.

The particles on the wires are considerably smaller (50-150 nm) than those that have grown on the substrate (about 300-500 nm). Prolonged current flow primarily enhances particle growth on the graphite substrate, likely due to the distinct materials and topologies of wires versus rough graphite. Similar substrate-dependent growth patterns have been observed on carbon nanofibers with different structural compositions. Platelet nanofibers exhibited superior platinum distribution compared to tubular counterparts, featuring smaller nanoparticles (up to 10 nm) with reduced coalescence and a highly nanostructured surface [53]. This enhanced performance was attributed to stronger catalyst anchoring in platelet morphologies, minimizing coalescence and maintaining well-dispersed, nanometer-sized catalyst particles. These observations underscore the critical role of substrate characteristics in nanoparticle growth.

The dendritic appearance (Figure 1f) of the particles becomes even more pronounced compared to Pt/AgNW (Figure 1b). Investigation into parameters used for metal doping such as exposure time and current density on platinum nanoparticle formation revealed that apart from current density the exposure time also encourages dendritic formation, resulting in more flower like structures [52]. The resulting larger effective precious metal surface area due to the nanostructured morphology may prove beneficial in terms of the hydrogen reaction kinetics.

Table 1. Kinetic parameters of the Pt loaded electrodes in 0.5 M H_2SO_4

			Pt/AgNW			
Pt loading (μg/cm^2)	5	14	26	52	126	
$E_{-10\ mA/cm^2}$ (mV)	-264	-231	-220	-195	-162	
Tafel slope (mV/dec)	-105	-97	-93	-90	-92	
			Pt/C			
Pt loading (μg/ cm^2)	5	13	19	63	101	136
$E_{-10\ mA/cm^2}$ (mV)	-387	-234	-81	-51	-42	-39
Tafel slope (mV/dec)	-160	-142	-57	-53	-49	-52
			Pt/AgNW/C			
Pt loading (μg/cm^2)	5	14	25	41	64	115
$E_{-10\ mA/cm^2}$ (mV)	-236	-116	-86	-72	-67	-43
Tafel slope (mV/dec)	-121	-68	-59	-60	-55	-52

To examine the roughness of the graphite substrate itself, CV measurements were performed to determine the electrochemical double layer capacitance. Figure 2 displays the recorded curves at different scan rates in a non-faradaic region where only double layer charging occurs. The double layer capacitance was calculated according to Eq. 2 with the scan rate v at a potential of 0.23 V vs. RHE [54].

$$C_{dl} = \frac{\delta Q}{\delta E} = \frac{idt}{dE} = \frac{i}{v} \tag{2}$$

By plotting half the difference between the positive and negative current densities for each scan rate, the double layer capacitance is determined as 153 μF. By comparing the obtained value with the capacitance of an ideal flat catalyst surface, which is usually assumed to be 0.02 mF/cm^2 [55] the surface of the graphite substrate exhibits a roughness

factor of about 7.7. This suggests that the graphite substrate offers a diverse range of surface areas with varying electronic properties, which might benefit the anchoring and growth properties of nanoparticles.

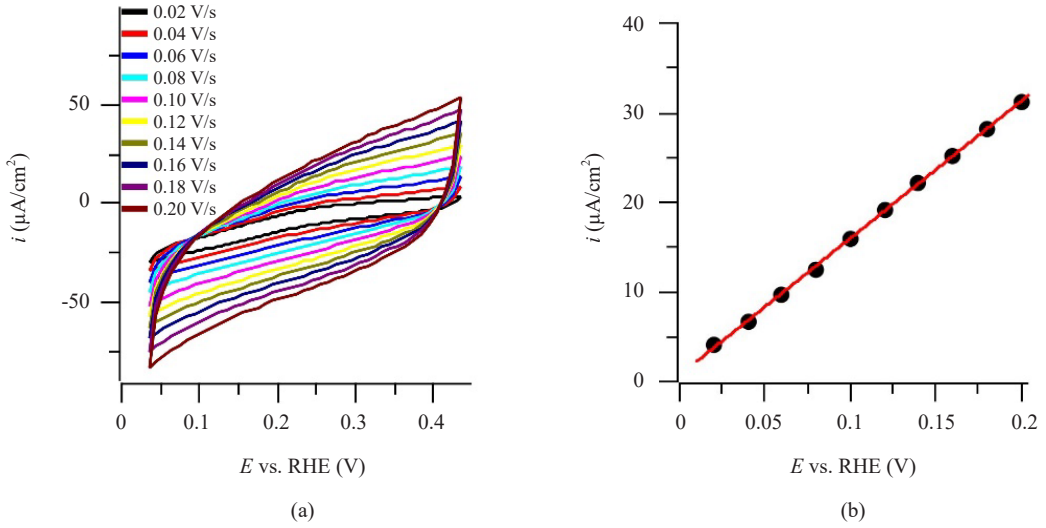

Figure 2. a) Cyclic voltammograms for the graphite substrate at different scan rates; b) dependence of the capacitive current density on the scan rate at 0.23 V vs. RHE

3.2 *Electrocatalytic HER activity*

Figure 3 shows the polarization curves for the different substrates with varying Pt loadings, corrected for the solution resistance. The solution resistance was estimated by measuring the high frequency resistance (HFR) of a platinum plate, which yielded a value of 0.8 $\Omega \cdot cm^2$ in the same cell configuration [56]. This ensures that the conductivity properties of the different electrode substrates (AgNW, C, AgNW/C) are not compensated and the electrocatalysis measurements reflect the activity of the electrode materials [57]. All Pt decorated electrodes display progressive electrocatalytic activity with increasing Pt loading. Their corresponding overpotentials required to drive a current of -10 mA/cm^2 are listed in Table 1.

The conductive AgNW network shows a good capability to promote hydrogen evolution with rising Pt content. In particular, a low loading of 5 $\mu g/cm^2$ results in a significant potential reduction of 238 mV at -2 mA/cm^2 relative to the pure AgNW network. However, it exhibits for loadings above 14 $\mu g/cm^2$ diminished catalytic activity in comparison to the graphite or the directly on the graphite substrate applied AgNWs. In the nanowire substrate, the current flow has to occur through the percolation network, whereby the sheet resistance of 6 Ω is particularly noticeable at higher current flows. Compared to the graphite based substrates, higher voltages are required for the same hydrogen formation rate.

The bare graphite and AgNW substrates show only a low catalytic activity towards HER, similar to bulk silver as predicted by the volcano plot, where the current exchange density is about 5 orders of magnitude lower than for platinum [58]. The Pt/C and Pt/AgNW/C demonstrate similar HER performance at higher loadings, which indicates that the AgNW network on the graphite substrate does not limit the substrate conductivity. This is in accordance with the SEM micrographs which illustrate that the particles tend to deposit uniformly on the wires and that no particular regions are preferentially occupied. At very small amounts of Pt, the Pt/AgNW and Pt/AgNW/C electrodes (5 and 14 $\mu g/cm^2$) evince markedly enhanced electrocatalytic activity compared to the AgNW free carbon substrates at nearly the same loadings (5 and 13 $\mu g/cm^2$). The highest Pt loaded carbon based electrode materials (136 $\mu g/cm^2$ and 115 $\mu g/cm^2$) need only a small overpotential of -39 mV and -43 mV, respectively, for a current density of -10 mA/cm^2. This performance is comparable to a commercial 20 wt% Pt/C electrode with an overpotential of approximately -29 mV [59].

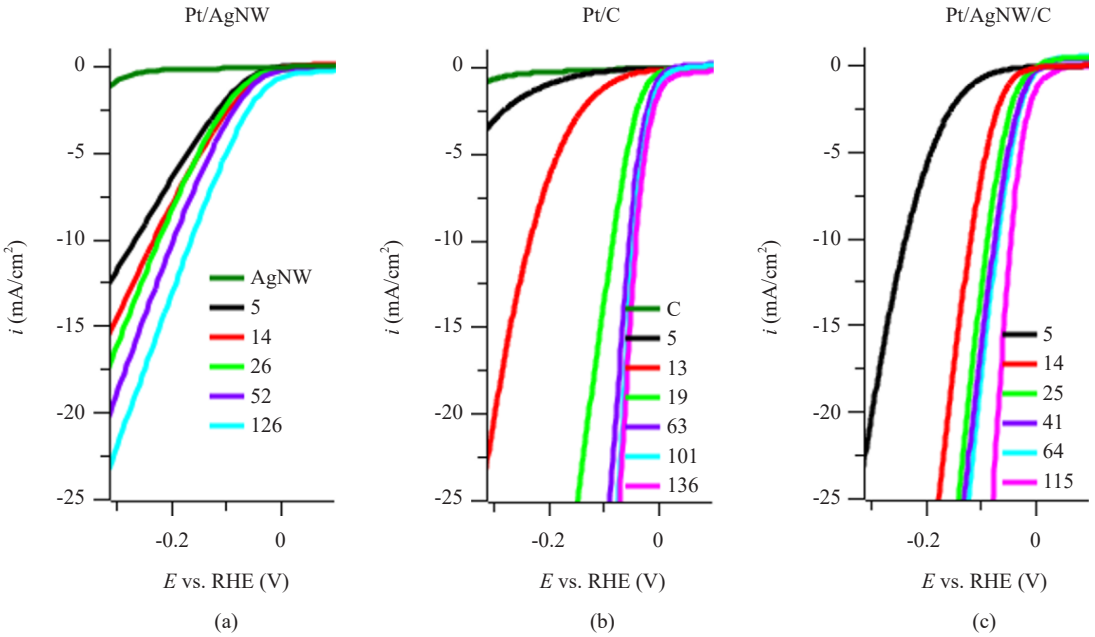

Figure 3. Polarization curves of the platinum decorated electrodes a) Pt/AgNW (5, 14, 26, 52, 126 µg/cm^2 Pt); b) Pt/C (5, 13, 19, 63, 101, 136 µg/cm^2 Pt); c) Pt/AgNW/C (5, 14, 25, 41, 64, 115 µg/cm^2 Pt)

The data demonstrate that as the Pt loading is increased, the overpotential undergoes a notable reduction (Figure 4). This trend is observed to be analogous in the case of the Pt loaded graphite and AgNW/C substrates. However, in the region of low Pt amounts an increase in Pt content from 5 to 26 µg/cm^2 results in a significant reduction of the overpotential. This increase in catalytic activity with platinum amount flattens significantly with loadings exceeding about 60 µg/cm^2. Beyond this point, further increases in platinum loading have only a minor impact on improving the catalytic performance. This suggests that a sufficient level of performance in relation to the precious metal used is already achieved around 60 µg/cm^2.

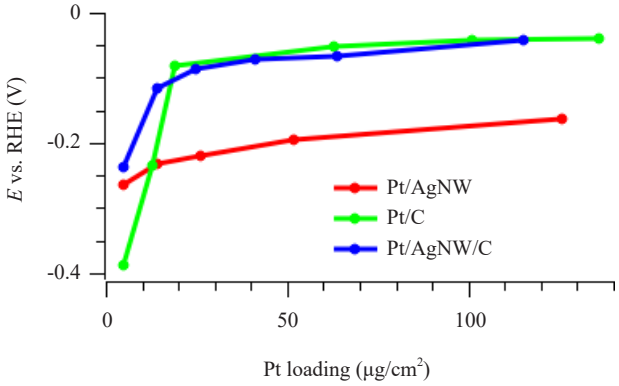

Figure 4. Overpotential at -10 mA/cm^2 as a function of the Pt loading

Looking at very small loadings (5 µg/cm^2) a strong effect of the silver nanowire network can be observed. Here, the Pt/C electrode exhibits the largest overpotential whereas the silver nanowires show the capability to reduce the overpotential by 121 mV in case of Pt/AgNW and 151 mV for Pt/AgNW/C. In the range of very small Pt loadings,

the presence of lower sized platinum nanoparticles is predominant, which facilitates a more substantial electronic impact of the silver on the platinum compared to larger platinum nanoparticle assemblies where the silver influence is insignificant. A synergistic effect was also observed for Pt nanoparticles deposited on AgNPs, where the overpotential at -10 mA/cm^2 was found to be decreased by 43 mV in comparison to bare PtNPs [49]. This effect was attributed to an improved proton affinity resulting from a more negative surface potential in the Pt satellites. It was thus concluded that the more electropositive silver core raises the Fermi level of Pt in Ag/Pt assemblies.

3.3 *Tafel analysis*

In acidic media, the formation of molecular hydrogen is a two step process involving three different reaction mechanisms. The initial Volmer reaction is associated with the discharge of the hydronium ion (H_3O^+) under the formation of a surface adsorbed hydrogen atom

$$H_3O^+ + e^- \rightarrow H_{ad} + H_2O$$

The next step is the formation of the hydrogen molecule, either according to a Heyrovsky reaction concomitant with electrochemical desorption

$$H_{ad} + H_3O^+ + e^- \rightarrow H_2 + H_2O$$

or to a Tafel reaction under recombination of two adsorbed hydrogen atoms

$$H_{ad} + H_{ad} \rightarrow H_2$$

The analysis of the Tafel slope can provide insights into the kinetic processes governing the rate determining step in a given current density dependent overpotential region. If the Volmer reaction is the rate determining step of the hydrogen evolution, the Tafel slope should be about -120 mV/dec, while a rate determining Tafel or Heyrovsky mechanism should result in slopes of about -30 and -40 mV/dec, respectively [60, 61].

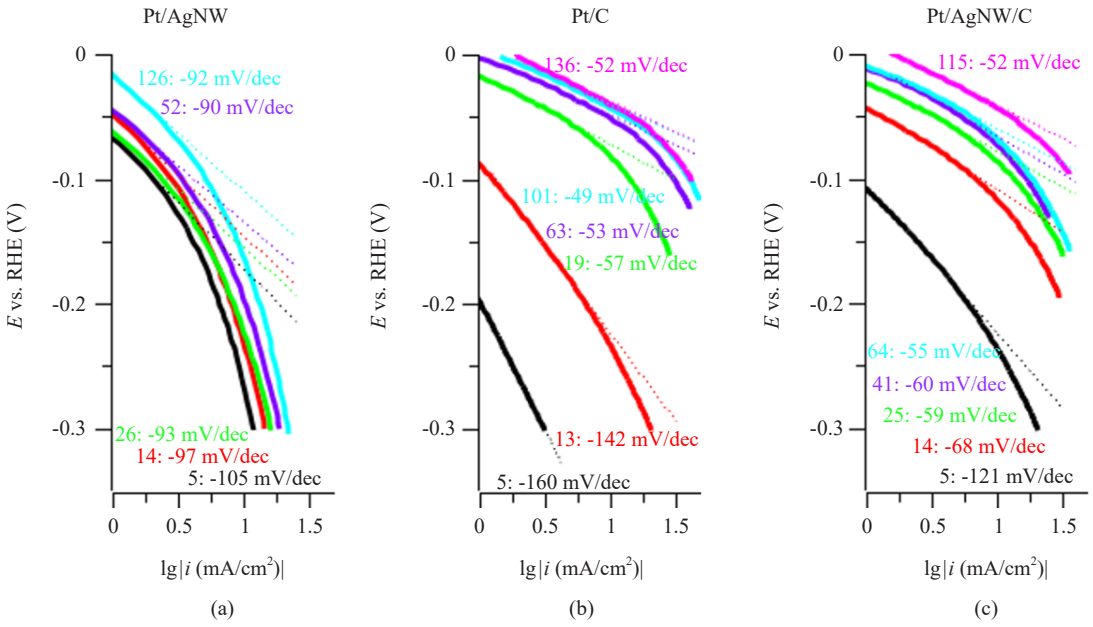

Figure 5. Tafel plots of the various electrodes (Pt loading in µg/cm^2): a) Pt/AgNW; b) Pt/C; c) Pt/AgNW/C

Pt/C electrodes with higher Pt loadings (63, 101 and 136 µg/cm^2) demonstrate Tafel slopes of approximately -52 mV/dec in the linear low overpotential region corresponding to -3 to -10 mA/cm^2 (Figure 5). These values align with those observed from the commercial 20 wt% Pt/C with -38.5 mV/dec [59]. These Tafel slope values indicate that the electrocatalysts follow a Volmer-Tafel mechanism with the rate determining Tafel step. This is characterized by a fast primary discharge step, followed by a slow recombination step due to low surface coverage by adsorbed hydrogen. Nevertheless, it has been evidenced that, up to -0.1 V vs. RHE, the Volmer-Heyrovsky mechanism also occurs and neither of the two mechanisms can be considered to be exclusively determining [62].

In the high overpotential region (current densities above -10 mA/cm^2), an increase in Tafel slopes occurs, reflecting the potential-dependent reaction rates of individual HER steps [63]. Higher overpotentials lead to increased surface coverage of adsorbed hydrogen atoms, resulting in the discharge step becoming rate determining, with a characteristic Tafel slope of -120 mV/dec [64]. Similar potential-dependent behavior was reported for bulk Pt disc electrodes, with Tafel slopes transitioning from -36 to -125 mV/dec in the high potential regime [65], aligning with the present findings.

The HER performance as well as the Tafel slopes of the electrodes investigated in the present work are in the range of previously reported results with PtNP doped electrodes using a carbon based substrate, such as a Pt loaded vertical graphene electrode with -47 mV at -10 mA/cm^2 and a Tafel slope of -27 mV/dec [66]. HER catalytic and Tafel parameters were also obtained for a Pt/pencil graphite electrode with -49 mV and -52 mV/dec [67] and for a platinum-doped nitrogenated porous two-dimensional C_2N structure with -60 mV and -33 mV/dec [68], respectively. These findings confirm that the investigated electrodes, which were fabricated using an easy to handle deposition technique, enable efficient electrocatalysis which can be even supported by silver nanowire structures.

4. Conclusion

PtNP decorated electrodes were fabricated via constant potential deposition on pristine graphite and silver nanowire networks coated on glass and graphite substrates. Varying the platinum loading demonstrated that hydrogen evolution is effectively catalysed from a loading level of approximately 60 µg/cm^2, requiring overvoltages of -51 mV (Pt/C) and -67 mV (Pt/AgNW/C) to achieve a current density of -10 mA/cm^2. Beyond this loading, performance improvements plateaued. Notably, AgNWs exhibited a significant effect at low Pt loadings (5 µg/cm^2) compared to Pt/C, likely due to differences in electrode morphology. This hypothesis is supported by observations of Pt shell formation comprising small agglomerates at short deposition times. A comparison with Pt/C revealed that extended current flow led to the growth of larger Pt particles on Pt/AgNW/C, reducing the nanowires' synergistic influence on HER catalysis. Kinetic Tafel analysis corroborated the excellent electrocatalytic activity, yielding slopes of approximately -52 mV/dec for both Pt/C and Pt/AgNW/C systems. These comprehensive electrochemical studies demonstrate that even minimal quantities of Pt enable efficient HER electrocatalysis, potentially enhanced by the synergistic effect of AgNWs.

Acknowledgement

The authors are grateful to Constanze Eulenkamp for her support with the scanning electron micrographs.

Conflict of interest

The corresponding author states that there is no conflict of interest. There was no specific funding for this project.

References

[1] Abdin Z, Zafaranloo A, Rafiee A, Mérida W, Lipiński W, Khalilpour KR. Hydrogen as an energy vector. *Renewable and Sustainable Energy Reviews*. 2020; 120: 109620. Available from: https://doi.org/10.1016/j.rser.2019.109620.

[2] Jiang R, Tung S, Tang Z, Li L, Ding L, Xi X, et al. A review of core-shell nanostructured electrocatalysts for

oxygen reduction reaction. *Energy Storage Materials*. 2018; 12: 260-276. Available from: https://doi.org/10.1016/j.ensm.2017.11.005.
[3] Guilbert D, Vitale G. Hydrogen as a clean and sustainable energy vector for global transition from fossil-based to zero-carbon. *Clean Technologies*. 2021; 3(4): 881-909. Available from: https://doi.org/10.3390/cleantechnol3040051.
[4] Dincer I. Green methods for hydrogen production. *International Journal of Hydrogen Energy*. 2012; 37(2): 1954-1971. Available from: https://doi.org/10.1016/j.ijhydene.2011.03.173.
[5] Ahrens F, Land J, Krumdieck S. Decarbonization of nitrogen fertilizer: a transition engineering desk study for agriculture in Germany. *Sustainability*. 2022; 14(14): 8564. Available from: https://doi.org/10.3390/su14148564.
[6] Pawar ND, Heinrichs HU, Winkler C, Heuser P, Ryberg SD, Robinius M, et al. Potential of green ammonia production in India. *International Journal of Hydrogen Energy*. 2021; 46(54): 27247-27267. Available from: https://doi.org/10.1016/j.ijhydene.2021.05.203.
[7] Harichandan S, Kar SK, Rai PK. A systematic and critical review of green hydrogen economy in India. *International Journal of Hydrogen Energy*. 2023; 48(81): 31425-31442. Available from: https://doi.org/10.1016/j.ijhydene.2023.04.316.
[8] Whitehead J, Newman P, Whitehead J, Lim KL. Striking the right balance: Understanding the strategic applications of hydrogen in transitioning to a net zero emissions economy. *Sustainable Earth Reviews*. 2023; 6(1): 1-10. Available from: https://doi.org/10.1186/s42055-022-00049-w.
[9] Song J, Wei C, Huang ZF, Liu C, Zeng L, Wang X, et al. A review on fundamentals for designing oxygen evolution electrocatalysts. *Chemical Society Reviews*. 2020; 49(7): 2196-2214. Available from: https://doi.org/10.1039/C9CS00607A.
[10] Hu C, Zhang L, Gong J. Recent progress made in the mechanism comprehension and design of electrocatalysts for alkaline water splitting. *Energy and Evironmental Science*. 2019; 12(9): 2620-2645. Available from: https://doi.org/10.1039/C9EE01202H.
[11] Devendra BK, Praveen BM, Tripathi VS, Nagaraju DH, Nayana KO. Hydrogen evolution reaction by platinum coating. *Iranian Journal of Science and Technology, Transactions A: Science*. 2021; 45: 1993-2000. Available from: https://doi.org/10.1007/s40995-021-01220-2.
[12] Zhang C, Xu L, Shan N, Sun T, Chen J, Yan Y. Enhanced electrocatalytic activity and durability of Pt particles supported on ordered mesoporous carbon spheres. *ACS Catalysis*. 2014; 4(6): 1926-1930. Available from: https://doi.org/10.1021/cs500107t.
[13] Cheng NC, Stambula S, Wang D, Banis MN, Liu J, Riese A, et al. Platinum single-atom and cluster catalysis of the hydrogen evolution reaction. *Nature Communications*. 2016; 7(1363): 1-9. Available from: https://doi.org/10.1038/ncomms13638.
[14] Grigoriev SA, Millet P, Fateev VN. Evaluation of carbon-supported Pt and Pd nanoparticles for the hydrogen evolution reaction in PEM water electrolysers. *Journal of Power Sources*. 2008; 177(2): 281-285. Available from: https://doi.org/10.1016/j.jpowsour.2007.11.072.
[15] Li Z, Ge R, Su J, Chen L. Recent progress in low Pt content electrocatalysts for hydrogen evolution reaction. *Advanced Materials Interfaces*. 2020; 7(14): 2000396. Available from: https://doi.org/10.1002/admi.202000396.
[16] Stephens IE, Chorkendorff I. Minimizing the use of platinum in hydrogen-evolving electrodes. *Angewandte Chemie International Edition*. 2011; 50(7): 1476-1477. Available from: https://doi.org/10.1002/anie.201005921.
[17] Huang X, Zeng Z, Bao S, Wang B, Qi X, Fan Z, et al. Solution-phase epitaxial growth of noble metal nanostructures on dispersible single-layer molybdenum disulfide nanosheets. *Nature Communications*. 2013; 4(1): 1444. Available from: https://doi.org/10.1038/ncomms2472.
[18] Xu GR, Hui JJ, Huang T, Chen Y, Lee JM. Platinum nanocuboids supported on reduced graphene oxide as efficient electrocatalyst for the hydrogen evolution reaction. *Journal of Power Sources*. 2015; 285: 393-399. Available from: https://doi.org/10.1016/j.jpowsour.2015.03.131.
[19] Chen H, Chen JT, Shao L, Wang L, Fu XZ, Luo JL. Minimum and well-dispersed platinum nanoparticles on 3D porous nickel for highly efficient electrocatalytic hydrogen evolution reaction enabled by atomic layer deposition. *Applied Surface Science*. 2019; 494: 1091-1099. Available from: https://doi.org/10.1016/j.apsusc.2019.07.251.
[20] Tan TL, Wang LL, Zhang J, Johnson DD, Bai K. Platinum nanoparticle during electrochemical hydrogen evolution: adsorbate distribution, active reaction species, and size effect. *ACS Catalysis*. 2015; 5(4): 2376-2383. Available from: https://doi.org/10.1021/cs501840c.
[21] Ma Z, Tian H, Meng G, Peng L, Chen Y, Chen C, et al. Size effects of platinum particles@CNT on HER and ORR performance. *Science China Materials*. 2020; 63(12): 2517-2529. Available from: https://doi.org/10.1007/s40843-

020-1449-2.
[22] Antolini E. Formation, microstructural characteristics and stability of carbon supported platinum catalysts for low temperature fuel cells. *Journal of Material Science*. 2003; 38: 2995-3005. Available from: https://doi.org/10.1023/A:1024771618027.
[23] Hotze EM, Phenrat T, Lowry GV. Nanoparticle aggregation: Challenges to understanding transport and reactivity in the environment. *Journal of Environmental Quality*. 2010; 39(6): 1909-1924. Available from: https://doi.org/10.2134/jeq2009.0462.
[24] Neuberger F, Baranyai J, Schmidt T, Cottre T, Kaiser B, Jaegermann W, et al. From bulk to atoms: the influence of particle and cluster size on the hydrogen evolution reaction. *Zeitschrift für Physikalische Chemie*. 2020; 234(5): 847-865. Available from: https://doi.org/10.1515/zpch-2019-1424.
[25] Jian C, Cai Q, Hong W, Li J, Liu W. Enhanced hydrogen evolution reaction of MoOx/Mo cathode by loading small amount of Pt nanoparticles in alkaline solution. *International Journal of Hydrogen Energy*. 2017; 42(27): 17030-17037. Available from: https://doi.org/10.1016/j.ijhydene.2017.05.223.
[26] Dominguez-Crespo MA, Ramírez-Meneses E, Torres-Huerta AM, Garibay-Febles V, Philippot K. Kinetics of hydrogen evolution reaction on stabilized Ni, Pt and Ni-Pt nanoparticles obtained by an organometallic approach. *International Journal of Hydrogen Energy*. 2012; 37(6): 4798-4811. Available from: https://doi.org/10.1016/j.ijhydene.2011.12.109.
[27] Fu M, Zhang Q, Sun Y, Ning G, Fan X, Wang H, et al. Ni-Fe nanocubes embedded with Pt nanoparticles for hydrogen and oxygen evolution reactions. *International Journal of Hydrogen Energy*. 2020; 45(41): 20832-20842. Available from: https://doi.org/10.1016/j.ijhydene.2020.05.170.
[28] Zainal SN, Sookhakian M, Woi PM, Alias Y. Ternary molybdenum disulfde nanosheets-cobalt oxide nanocubes-platinum composite as efficient electrocatalyst for hydrogen evolution reaction. *Electrochimica Acta*. 2020; 345: 136255. Available from: https://doi.org/10.1016/j.electacta.2020.136255.
[29] Mariandry K, Kokate R, Somerville SV, Gloag L, Cheong S, Carroll LR, et al. Controlling platinum active sites on silver nanoparticles for hydrogen evolution reaction. *Chemistry of Materials*. 2020; 35(20): 8636-8644. Available from: https://doi.org/10.1021/acs.chemmater.3c01765.
[30] Hou D, Zhou W, Liu X, Zhou K, Xie J, Li G, et al. Pt nanoparticles/MoS_2 nanosheets/carbon fibers as efficient catalyst for the hydrogen evolution reaction. *Electrochimica Acta*. 2015; 166: 26-31. Available from: https://doi.org/10.1016/j.electacta.2015.03.067.
[31] Chang J, Feng L, Liu C, Xing W, Hu X. Ni_2P enhances the activity and durability of the Pt anode catalyst in direct methanol fuel cells. *Energy and Environmental Science*. 2014; 7(5): 1628-1632. Available from: https://doi.org/10.1039/C4EE00100A.
[32] Liu M, Zhang R, Chen W. Graphene-supported nanoelectrocatalysts for fuel cells: synthesis, properties, and applications. *Chemical Reviews*. 2014; 114(10): 5117-5160. Available from: https://doi.org/10.1021/cr400523y.
[33] Guo S, Dong S, Wang E. Constructing carbon nanotube/Pt nanoparticle hybrids using an imidazolium-salt-based ionic liquid as a linker. *Advanced Materials*. 2010; 22(11): 1269-1272. Available from: https://doi.org/10.1002/adma.200903379.
[34] Bessel CA, Laubernds K, Rodriguez NM, Baker RTK. Graphite nanofibers as an electrode for fuel cell applications. *The Journal of Physical Chemistry B*. 2001; 105(6): 1115-1118. Available from: https://doi.org/10.1021/jp003280d.
[35] Hao J, Wei F, Zhang X, Li L, Zhang C, Liang D, et al. Defect and doping engineered penta-graphene for catalysis of hydrogen evolution reaction. *Nanoscale Research Letters*. 2021; 16: 1-9. Available from: https://doi.org/10.1186/s11671-021-03590-3.
[36] Li Y, Wang S, Hu Y, Zhou X, Zhang M, Jia X, et al. Highly dispersed Pt nanoparticles on 2D MoS_2 nanosheets for efficient and stable hydrogen evolution reaction. *Journal of Materials Chemistry A*. 2022; 10(10): 5273-5279. Available from: https://doi.org/10.1039/D1TA10725A.
[37] Zhang Y, Tan J, Wen F, Zhou Z, Zhu M, Yin S, et al. Platinum nanoparticles deposited nitrogen-doped carbon nanofiber derived from bacterial cellulose for hydrogen evolution reaction. *International Journal of Hydrogen Energy*. 2018; 43(12): 6167-6176. Available from: https://doi.org/10.1016/j.ijhydene.2018.02.054.
[38] Qian L, Hu H, Zheng Y, Zhu Y, Dai Y, Zhang T, et al. Platinum nanoparticles anchored on flowerlike zinc oxide nanosheet array electrocatalysts for efficient hydrogen evolution reaction. *ACS Applied Nano Materials*. 2023; 6(21): 19818-19826. Available from: https://doi.org/10.1021/acsanm.3c03629.
[39] Yan X, Li H, Sun J, Liu P, Zhang H, Xu B, et al. Pt nanoparticles decorated high-defective graphene nanospheres as highly efficient catalysts for the hydrogen evolution reaction. *Carbon*. 2018; 137: 405-410. Available from: https://doi.org/10.1016/j.carbon.2018.05.046.

[40] Li W, Zhang Z, Zhang W, Zou S. MoS_2 nanosheets supported on hollow carbon spheres as efficient catalysts for electrochemical hydrogen evolution reaction. *ACS Omega*. 2017; 2(8): 5087-5094. Available from: https://doi.org/10.1021/acsomega.7b00755.
[41] Bernsmeier D, Sachse R, Bernicke M, Schmack R, Kettemann F, Polte J, et al. Outstanding hydrogen evolution performance of supported Pt nanoparticles: Incorporation of preformed colloids into mesoporous carbon films. *Journal of Catalysis*. 2019; 369: 181-189. Available from: https://doi.org/10.1016/j.jcat.2018.11.006.
[42] Zhang H, Noonan O, Huang X, Yang Y, Xu C, Zhou L, et al. Surfactant-free assembly of mesoporous carbon hollow spheres with large tunable pore sizes. *ACS Nano*. 2016; 10(4): 4579-4586. Available from: https://doi.org/10.1021/acsnano.6b00723.
[43] Zellner D, Varga A, Schwager M. Effect of morphological changes due conductivity enhancing post treatment on the absorption and photoluminescence of AgNW thin films. *Journal of Nano Research*. 2023; 81: 9-20. Available from: https://doi.org/10.4028/p-AiIhP6.
[44] Choo DC, Kim TW. Degradation mechanisms of silver nanowire electrodes under ultraviolet irradiation and heat treatment. *Scientific Reports*. 2017; 7(1): 1696. Available from: https://doi.org/10.1038/s41598-017-01843-9.
[45] Hansen JN, Prats H, Toudahl KK, Mørch Secher N, Chan K, Kibsgaard J, et al. Is there anything better than Pt for HER? *ACS Energy Letters*. 2021; 6(4): 1175-1180. Available from: https://doi.org/10.1021/acsenergylett.1c00246.
[46] Muench F. Electroless plating of metal nanomaterials. *ChemElectroChem*. 2021; 8(16): 2993-3012. Available from: https://doi.org/10.1002/celc.202100285.
[47] Liu Y, Wang Q, Zhang J, Ding J, Cheng Y, Wang T, et al. Recent advances in carbon-supported noble-metal electrocatalysts for hydrogen evolution reaction: syntheses, structures, and properties. *Advanced Energy Materials*. 2022; 12(28): 2200928. Available from: https://doi.org/10.1002/aenm.202200928.
[48] Gulumian M, Andraos C, Afantitis A, Puzyn T, Coville NJ. Importance of surface topography in both biological activity and catalysis of nanomaterials: can catalysis by design guide safe by design? *International Journal of Molecular Sciences*. 2021; 22(15): 8347. https://doi.org/10.3390/ijms22158347.
[49] Yang L, Grzeschik R, Jiang P, Yu L, Hu C, Du A, et al. Tuning the electronic properties of platinum in hybrid-nanoparticle assemblies for use in hydrogen evolution reaction. *Angewandte Chemie International Edition*. 2023; 62(25): e202301065. Available from: https://doi.org/10.1002/anie.202301065.
[50] Shigihara Y, Ooi A, Tada E, Nishikata A. Dissolution and consequent morphological evolution of electrodeposited Pt-Cu nanoparticles under potential cycling in 0.5 M H_2SO_4 solution. *Journal of The Electrochemical Society*. 2019; 166(11): C3170. Available from: https://doi.org/10.1149/2.0221911jes.
[51] Dhanasekaran P, Lokesh K, Ojha PK, Sahu AK, Bhat SD, Kalpana D. Electrochemical deposition of three-dimensional platinum nanoflowers for high-performance polymer electrolyte fuel cells. *Journal of Colloid and Interface Science*. 2020; 572: 198-206. Available from: https://doi.org/10.1016/j.jcis.2020.03.078.
[52] Dhanasekaran P, Rajavarman S, Selvaganesh SV, Bhat SD. Insight towards nucleation mechanism and change in morphology for nanostructured platinum thin film directly grown on carbon substrate via electrochemical deposition. *Materials*. 2021; 14(9): 2330. Available from: https://doi.org/10.3390/ma14092330.
[53] Salernitan E, Giorgi L, Makris TD. Direct growth of carbon nanofibers on carbon-based substrates as integrated gas diffusion and catalyst layer for polymer electrolyte fuel cells. *International Journal of Hydrogen Energy*. 2014; 39(27): 15005-15016. Available from: https://doi.org/10.1016/j.ijhydene.2014.07.060.
[54] McCrory CCL, Jung S, Peters JC, Jaramillo TF. Benchmarking heterogeneous electrocatalysts for the oxygen evolution reaction. *Journal of the American Chemical Society*. 2013; 135: 16977-16987: Available from: https://doi.org/10.1021/ja407115p.
[55] Ge Y, Xie X, Roscher J, Holze R, Qu Q. How to measure and report the capacity of electrochemical double layers, supercapacitors, and their electrode materials. *Journal of Solid State Electrochemistry*. 2020; 24: 3215-3230. Available from: https://doi.org/10.1007/s10008-020-04804-x.
[56] Zheng W. IR compensation for electrocatalysis studies: Considerations and recommendations. *ACS Energy Letters*. 2023; 8(4): 1952-1958. Available from: https://doi.org/10.1021/acsenergylett.3c00366.
[57] Chung DY, Park S, Lopes PP, Stamenkovic VR, Sung YE, Markovic NM, et al. Electrokinetic analysis of poorly conductive electrocatalytic materials. *ACS Catalysis*. 2020; 10(9): 4990-4996. Available from: https://doi.org/10.1021/acscatal.0c00960.
[58] Cook TR, Dogutan DK, Reece SY, Surendranath Y, Teets TS, Nocera DG. Solar energy supply and storage for the legacy and nonlegacy worlds. *Chemical Reviews*. 2010; 110(11): 6474-6502. Available from: https://doi.org/10.1021/cr100246c.
[59] Cai ZX, Wang ZL, Xia YJ, Lim H, Zhou W, Taniguchi A, et al. Tailored catalytic nanoframes from metal-organic

frameworks by anisotropic surface modification and etching for the hydrogen evolution reaction. *Angewandte Chemie*. 2020; 133(9): 4797-4805. Available from: https://doi.org/10.1002/ange.202010618.
[60] Conway BE, Tilak BV. Interfacial processes involving electrocatalytic evolution and oxidation of H_2, and the role of chemisorbed H. *Electrochimica Acta*. 2002; 47(22-23): 3571-3594. Available from: https://doi.org/10.1016/S0013-4686(02)00329-8.
[61] Pentland N, Bockris JO'M, Sheldon E. Hydrogen evolution reaction on copper, gold, molybdenum, palladium, rhodium, and iron: mechanism and measurement technique under high purity conditions. *Journal of The Electrochemical Society*. 1957; 104(3): 182. Available from: https://doi.org/10.1149/1.2428530.
[62] Watzele S, Fichtner J, Garlyyev B, Schwämmlein JN, Bandarenka AS. On the dominating mechanism of the hydrogen evolution reaction at polycrystalline Pt electrodes in acidic media. *ACS Catalysis*. 2018; 8(10): 9456-9462. Available from: https://doi.org/10.1021/acscatal.8b03365.
[63] Lasia A. Mechanism and kinetics of the hydrogen evolution reaction. *International Journal of Hydrogen Energy*. 2019; 44(36): 19484-19518. Available from: https://doi.org/10.1016/j.ijhydene.2019.05.183.
[64] Shinagawa T, Garcia-Esparza AT, Takanabe K. Insight on Tafel slopes from a microkinetic analysis of aqueous electrocatalysis for energy conversion. *Scientific Reports*. 2015; 5(1): 13801. https://https://doi.org/10.1038/srep13801.
[65] Conway BE, Bai L. Determination of adsorption of OPD H species in the cathodic hydrogen evolution reaction at Pt in relation to electrocatalysis. *Journal of Electroanalytical Chemistry and Interfacial Electrochemistry*. 1986; 198(1): 149-175. Available from: https://https://doi.org/10.1016/0022-0728(86)90033-1.
[66] Scremin J, Dos Santos IVJ, Hughes JP, Ferrari AGM, Valderrama E, Zheng W, et al. Platinum nanoparticle decorated vertically aligned graphene screen-printed electrodes: electrochemical characterisation and exploration towards the hydrogen evolution reaction. *Nanoscale*. 2020; 12(35): 18214-18224. Available from: https://doi.org/10.1039/D0NR04336B.
[67] Balint LC, Hulka I, Kellenberger A. Pencil graphite electrodes decorated with platinum nanoparticles as efficient electrocatalysts for hydrogen evolution reaction. *Materials*. 2021; 15(1): 73. Available from: https://doi.org/10.3390/ma15010073.
[68] Mahmood J, Li F, Jung SM, Okyay MS, Ahmad J, Kim SJ, et al. An efficient and pH-universal ruthenium-based catalyst for the hydrogen evolution reaction. *Nature Nanotechnology*. 2017; 12: 441-446. Available from: https://doi.org/10.1038/nnano.2016.304.